Scientia Iranica B (2015) 22(5), 1877–1890

Sharif University of Technology
Scientia Iranica
*Transactions B: Mechanical Engineering*
www.scientiairanica.com

# Lattice Boltzmann simulation of three-dimensional capsule deformation in a shear flow with different membrane constitutive laws

**Z. Hashemi[a], M. Rahnama[a,*] and S. Jafari[b]**

a. *Department of Mechanical Engineering, Faculty of Engineering, Shahid Bahonar University of Kerman, Kerman, P.O. Box 76169-13, Iran.*
b. *Department of Petroleum Engineering, Faculty of Engineering, Shahid Bahonar University of Kerman, Kerman, P.O. Box 76169-13, Iran.*

Received 27 October 2014; received in revised form 14 December 2014; accepted 3 February 2015

**KEYWORDS**
Lattice Boltzmann method;
Immersed boundary method;
Capsule deformation;
Shear flow;
Finite element method.

**Abstract.** In this paper, the deformation of an elastic spherical capsule suspended in a shear flow is studied in detail using Lattice Boltzmann method for fluid flow simulation, immersed boundary method for fluid-membrane interaction and finite element method for membrane force analysis. While Lattice Boltzmann method is capable of implementing inertia effects, computations were carried out for small Reynolds number in which inertia effects are negligible. Effects of three membrane constitutive equations on capsule deformation, including Neo-Hookean, zero-thickness shell approximation and Skalak's law with different area-dilation modulus, are studied in detail. Results presented in the form of Taylor deformation parameter, inclination angle and period of tank-treading motion of capsule, show close agreement between those obtained from Neo-Hookean and zero-thickness shell approximation with previous published ones. Such agreement is partially observed for Skalak's law implementing different area-dilation modulus. In general, behaviors of all three constitutive laws are similar for nondimensional shear rates of less than 0.05 while some differences were observed for its values of 0.1 and 0.2. As an efficient computational framework, it is shown that combined Lattice Boltzmann, Immersed Boundary and Finite element method is a promising method for such flow configuration, implementing different membrane constitutive laws.



## 1. Introduction

Deformation of a spherical capsule under shear flow has been a subject of research for more than three decades due to its physical complexity as well as its importance in many applications such as motion of red blood cell in blood flow and artificial capsules in food industries. Consisting of a thin elastic membrane with an incompressible fluid inside, a capsule starts to deform under shear flow with its final configuration depending on Reynolds number and shear rate. The complexity of such flow configuration stems from simultaneous implementation of Eulerian description for fluid flow, Lagrangian description of membrane deformation and their interconnection through a fluid-membrane interaction model.

Among the pioneers in investigating deformation of a capsule freely suspended in a shear flow, Barthès-Biesel and Rallison [1] derived the equations governing time-dependent deformation of membrane resulting from viscous stresses more than three decades ago. Their study was limited to a spherical capsule with

*. *Corresponding author. Tel.: +98 343 2111763; Fax: +98 343 2120964*
*E-mail address: rahnama@uk.ac.ir (M. Rahnama)*

small departure from sphericity. Substantial progress in computational methods and computer hardware, in the last few decades, created an opportunity to study three dimensional time-dependent capsule deformation in shear flow extensively [2-5]. A comprehensive review of these progresses was reported by Barthès-Biesel [6], in 2011, in which different modeling strategies in simulation of a spherical capsule suspended in a shear flow were presented along with their limitations and advantages. Progress in implementation of different viscosities for fluids inside and outside of the capsule membrane [4,7] and membrane constitutive laws and membrane bending resistance [8,9] are also reviewed in this paper.

Analytical methods based on perturbation solution for deformation of an initially spherical capsule in weak simple shear flow were presented by Barthès-Biesel and Rallison [1] and Barthès-Biesel [10]. These methods are limited to small deformations at Stokes flow regimes. On the other hand, computational methods are capable of representing details of flow and capsule deformation in three dimensions for large deformation, considering the effect of changing parameters such as different membrane constitutive models and fluid viscosities. Boundary Element Method (BEM) [2-5], Finite Difference Method (FDM) [7,11,12] and Lattice Boltzmann Method (LBM) [13-17] are among frequently used computational methods in simulation of capsule deformation in shear flow. BEM was the first successful method in revealing detailed physics of capsule deformation since two decades ago. Pozrikidis [2,9,18], Kraus et al. [19], Ramanujan and Pozrikidis [4], Navot and Sackler [20], Diaz et al. [21], Barthès-Biesel et al. [22] and Lac et al. [5] used BEM in their simulation, and their results were in close agreement with experimental data of Chang and Olbricht [23] and Walter et al. [24,25]. In their investigations, Ramanujan and Pozrikidis [4] studied the effect of large capsule deformation and fluid viscosity in detail for the first time. In spite of their great success, BEM simulation of capsule deformation suffered from a limitation regarding flow regime: BEM application is limited to Stokes flow where the effect of inertia is neglected, and also the full dynamics of capsules with complex geometries, such as biconcave capsules, cannot be handled due to instabilities in computations.

There are some applications for which fluid inertia effect has to be considered, such as artificial capsules in food and polymer processes. Moreover, the background fluid might be viscoelastic as is the case in biological flows which might not be simulated using BEM. These limitations motivated researchers to employ alternative methods among which there are finite difference of Navier-Stokes equations [7,11,12], and LBM with Immersed Boundary Method (IBM) [26,27] for fluid-particle interaction. Meanwhile, IBM has been used in simulation of many problems, such as deformation of elastic membranes. Eggleton and Popel [28] studied large deformation of capsules in shear flow using IBM; however, due to computational costs, simulations were carried out on a coarse mesh for a short period of time. Li and Sarkar [12] employed a front tracking method to simulate deformation of a spherical capsule in shear flow, and compared and discussed the performance of the method with the results obtained from BEM. Their results showed that, in spite of low-order surface stress calculations, the front tracking method is compared very well with high-order BEMs in predicting capsule deformation, orientation, and tank-treading motions.

Recently, LBM has emerged as a useful method for simulation of fluid-particle interaction problems due to some of its intrinsic features, such as fixed Eulerian grid and computational efficiency [29], as experienced by Hashemi et al. in particle flow simulation [30-32]. A combination of IBM and LBM was used by Feng and Michaelides [33,34] to study particulate flow. Based on progresses in combined IB-LBM method, Sui et al. [13-16] proposed a hybrid method consisting of IB-LBM and Finite Element Method (FEM) to study the deformation of a capsule in simple shear flow. In their earlier simulations, Sui et al. [13] used multi-block strategy to refine the mesh near the capsule to increase the accuracy and efficiency of computation. They used a finite element method to obtain forces acting on the membrane nodes of the three-dimensional capsule which was discretized into flat triangular elements. Compared with other published results in the literature, it was shown that this method is capable of predicting dynamic behavior of deformable capsules accurately. Sui et al. [13] studied deformation of initially spherical and oblate-spheroidal capsules with various membrane constitutive laws under shear flow where it was observed that there were good agreements between previous theory and numerical results. It was reported in their paper that the inertia effects were found to have significant impact on capsule deformation. Moreover, the unsteady tank-treading motion, in which the capsule undergoes periodic shape deformation and inclination oscillation while its membrane is rotating around the liquid inside, was revealed for the first time in simulations using IB-LBM. Later on, Sui et al. [16] coupled front-tracking method with the LBM to investigate the effect of different viscosities for fluids inside and outside of the membrane. These two fluids were treated as one fluid with varying physical properties in LBM simulation. Their computation of Taylor deformation parameter (defined in Section 3), capsule inclination angle and the tank-treading frequency showed good correspondence with previously published numerical results.

More recently, Kruger et al. [17] studied capsule deformation in shear flow using IB-LBM with FEM used for obtaining membrane forces from its deformation in the limiting case of small deformation where the analytical expressions were reported. Their main objective was to show the influence of mesh tessellation method, the spatial resolution, and the discrete delta function of the immersed boundary method on the numerical results. They came to the conclusion that details of the membrane mesh, as tessellation method and resolution, play only a minor role while the hydrodynamic resolution, i.e. the width of the discrete delta function, can significantly influence the accuracy of the simulations. Their study also showed that LBM is capable of reducing the computational time for simulation of deformable object immersed in a fluid while maintaining high accuracy.

The present study was performed using combined IBM, LBM and FEM for capsule deformation under a shear flow. While physics of such flow configuration has been matured in recent years as mentioned in the above literature review, there are still some issues which have not been addressed clearly in this computational framework such as the effect of different membrane constitutive equations on capsule deformation parameters such as length of major axis and area changes of capsule during its deformation as well as computational time. The first aim of the present paper is to compare the computational efficiency and accuracy of the combined method with other available techniques. Then the dynamic response of three different membrane constitutive laws namely zero-thickness shell formulation, Neo-Hookean law and Skalak's law at different shear rates are studied. Since the biological cells tend to deform at constant area, the area change during the deformation is an important factor. In the present work the resistance of different constitutive equations to area change under different conditions is also verified. Following the Skalak's law, the area dilation modulus controls the changes in area during the deformation. When this modulus approaches infinity, the area will be constant. The effects of different area dilation modulus are studied here to find a value which is appropriate for dynamic behavior of biological cells. The paper starts with a description of LBM for fluid flow simulation, IBM for fluid-capsule interaction modeling and FEM which is used for obtaining membrane forces from its deformation. In the results part of the paper, authors express their findings regarding the computational strategies, comparison of different membrane constitutive laws and major axes lengths and capsule area variations in more details compared to the previous published papers.

## 2. Numerical method

In order to study deformation of a spherical capsule in a shear flow, a combined computational frame, capable of simulating fluid motion, capsule membrane deformation and fluid-membrane interaction is required. In the present computations, a combination of three methods is used for such simulation composed of Lattice Boltzmann method for fluid flow simulation, immersed boundary method which models fluid-membrane interactions, and finite element method for computation of membrane forces from its deformation. In the following subsections, each of the above mentioned methods is described in more details.

### 2.1. Lattice Boltzmann method

Lattice Boltzmann method is a particle-based kinetic method which uses a mesoscopic approach for fluid flow computations. It is based on the numerical solution of Boltzmann equation from which velocity distribution function is obtained. The discretized form of this equation, using single relaxation time approximation (BGK model) [35], is expressed as:

$$f_\alpha(x + e_\alpha \delta t, t + \delta t) - f_\alpha(x, t) = -\frac{1}{\tau}[f_\alpha(x,t) - f_\alpha^{eq}(x,t)] + \delta t F_\alpha, \tag{1}$$

where $f_\alpha(x,t)$ is velocity distribution function in $\alpha$th discrete velocity direction; $x$ is the spatial position vector; $t$ is time; $\tau$ is the relaxation time; $f_\alpha^{eq}(x,t)$ is equilibrium velocity distribution function; and $F_\alpha$ is the external force. Different discretizations of three dimensional velocity vector have been proposed, however, the most widely used one is nineteen-velocity model which is called $D_3Q_{19}$, as shown in Figure 1. Discrete velocity sets $\{e_\alpha\}$ can be defined in this model as:

$$e_0 = (0,0,0),$$

$$e_\alpha = (\pm 1, 0, 0)c, (0, \pm 1, 0)c, (0, 0, \pm 1)c \quad \text{for} \quad \alpha = 1 \sim 6,$$

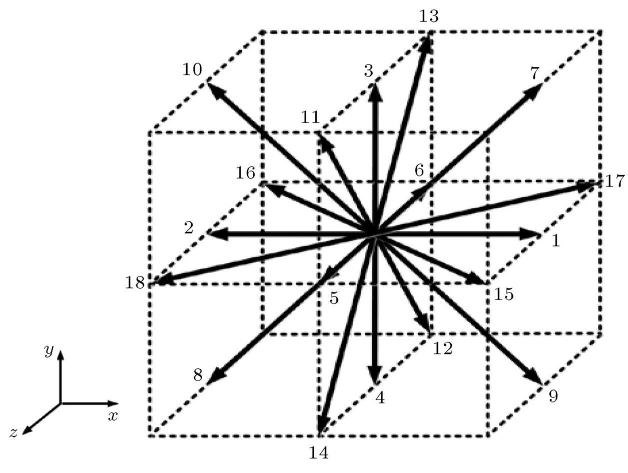


**Figure 1.** Velocity discretization in three-dimensional LB method: $D_3Q_{19}$ model.

$$e_\alpha = (\pm 1, \pm 1, 0)c, (0, \pm 1, \pm 1)c, (\pm 1, 0, \pm 1)c \quad \text{for} \quad \alpha = 7 \sim 18, \tag{2}$$

where $c = \delta x/\delta t$ is the lattice speed. The equilibrium distribution function can be expressed as:

$$f_\alpha^{eq} = \omega_\alpha \rho \left[ 1 + \frac{3\vec{e}_\alpha.\vec{u}}{c^2} + \frac{9\,(\vec{e}_\alpha.\vec{u})^2}{2c^4} - \frac{3\,(\vec{u}.\vec{u})}{2c^2} \right]. \tag{3}$$

The coefficients $\omega_\alpha$ are weighting factors that depends on the discrete velocity set in three spatial dimensions. In $D_3Q_{19}$ model, $\omega_0 = 1/3$ and $\omega_\alpha = 1/18$ for $\alpha = 1$ to 6, and $\omega_\alpha = 1/36$ for $\alpha = 7$ to 18.

Macroscopic variables such as density and velocity can be obtained from velocity distribution function as follows:

$$\rho = \sum f_\alpha, \tag{4}$$

$$\rho \vec{u} = \sum \vec{e}_\alpha f_\alpha. \tag{5}$$

Fluid viscosity is related to the relaxation time in LBM as $\upsilon = (\tau - 0.5)c_s^2 \delta t$, where $c_s$ is the lattice speed of sound and is equals to $c/\sqrt{3}$. External force term, which is introduced in the present LBM, is based on the method of Luo [36], which is expressed as:

$$F_\alpha = -3\omega_\alpha \rho e_\alpha . f/c^2. \tag{6}$$

Here $f$ is external force density at Eulerian nodes which is more discussed in Sections 2.2 and 2.3.

### *2.2. Immersed boundary method*

Immersed boundary method was initially developed by Peskin [26] in 1970s to model blood flow in the human heart. In this method, the effect of an object on fluid flow is specified by adding a body force to momentum equations. It can be explained using a set of fixed fluid Eulerian nodes, $x$, and moving Lagrangian points $s$ with position vectors $X(s,t)$, for membrane, see Figure 2. At each time step, a force $F(s,t)$ is computed for each membrane node due to its deformations. This Lagrangian force which is computed using a procedure explained in Section 2.3, is distributed on the Eulerian points by the following Dirac delta function interpolation:

$$f(x,t) = \sum_s F(s,t)\delta(\mathbf{x} - \mathbf{X}(s,t)). \tag{7}$$

For three-dimensional cases the discrete delta function can be written as:

$$\delta(x - X(s,t)) = \delta(x - X(s,t))\delta(y - Y(s,t))\delta(z - Z(s,t)), \tag{8}$$

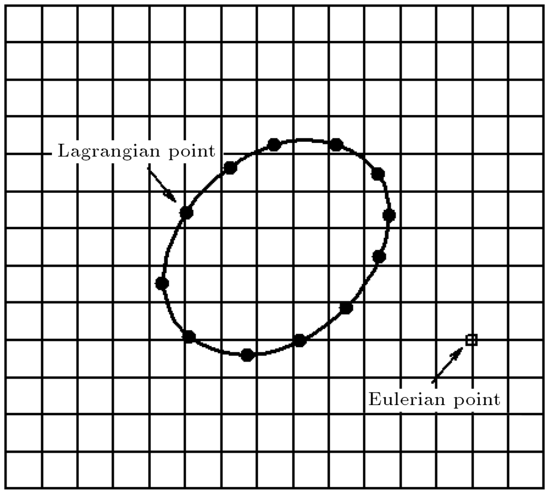


**Figure 2.** Schematic diagram showing fluid Eulerian and membrane Lagrangian points.

where for example,

$$\delta(x - X(s,t)) = \begin{cases} 1 - |x - X(s,t)| & |x - X(s,t)| \le 1 \\ 0 & \text{otherwise} \end{cases} \tag{9}$$

The new velocities of membrane Lagrangian nodes can be obtained from the local fluid velocities, $u(x,t)$, by the same interpolation function used in Eq. (7):

$$U(s,t) = \sum_x u(x,t)\delta(x - X(s,t)). \tag{10}$$

At the surface of the particle, the no-slip boundary condition is satisfied by equating boundary-node velocities with velocity obtained from its adjacent fluid nodes expressed as:

$$\frac{\partial X(s,t)}{\partial t} = u(X(s,t),t). \tag{11}$$

### *2.3. Membrane model: finite element method*

In order to compute elastic forces on membrane nodes, an appropriate constitutive equation, which describes the membrane properties, is required. Among different constitutive equations, the Neo-Hookean (NH) law is the simplest one with the strain energy function in the form of:

$$W^{\mathrm{NH}} = \frac{E_s}{6}\left( \lambda_1^2 + \lambda_2^2 - 3 + \frac{1}{\lambda_1^2 \lambda_2^2} \right), \tag{12}$$

in which $E_s$ is the surface shear elasticity modulus and $\lambda_1$ and $\lambda_2$ are the principle stretch ratios. The NH constitutive equation models membrane as a volume-incompressible isotropic material which means any increase in the area of membrane due to its deformation accompany with thinning of membrane thickness to preserve membrane volume. Another version of NH law is Zero-Thickness (ZT) shell formulation which was used by Ramanujan and Pozrikidis [4]. Here, a strain-energy function is expressed as:

$$W^{\mathrm{ZT}} = \frac{E_s}{6}\left[\lambda_1^2 + \lambda_2^2 - 2 - \log(\lambda_1^2\lambda_2^2) + \frac{1}{2}\log^2(\lambda_1^2\lambda_2^2)\right]. \tag{13}$$

Skalak et al. [37] proposed another constitutive equation, denoted by SK, to describe elastic behavior of red blood cells. A red blood cell tends to deform easily at constant area. In the SK law, the resistance of the membrane to area changes is represented by coefficient $C$ in its equation which is written as follow:

$$W^{\mathrm{SK}} = \frac{E_s}{12}\left[(\lambda_1^4 + \lambda_2^4 - 2\lambda_1^2 - 2\lambda_2^2 + 2) + C(\lambda_1^2\lambda_2^2 - 1)^2\right]. \tag{14}$$

The first term on the right-hand side of the above equation describes the shear effects, and the second term represents the area dilation. A membrane with zero change in area is obtained if $C$ approaches infinity.

The current study was done using finite element method developed by Charrier et al. [38] and Shrivastava and Tang [39] from which elastic forces of membrane nodes are obtained from their deformation, taking into account the selected constitutive law. Membrane surface is discretized using flat triangular elements which remain flat after deformation. The procedure of generating unstructured mesh on the surface of the membrane is presented in Section 3. This idealization allows us to employ in-plane-membrane theory for each element. To obtain element deformation, each individual undeformed triangular element is transferred to the plane of the deformed element (see Figure 3). Such pure displacement does not affect nodal forces of the element. Assuming constant displacement gradients within the element, displacement of any point on the surface of element can be expressed as:

$$u = \sum_{i=1}^{3} N_i u_i,$$

in which $N_i$ is the linear shape function defined as $N_i = \alpha_i x + \beta_i y + \gamma_i$ for each node $i$. The unknown coefficients in this function can be obtained by the fact that $N_i = 1$ at node $i$ and $N_i = 0$ at two other nodes. By virtue of this assumption, the displacement gradients and corresponding principal stretch ratios can be immediately determined [38]. Using the principle of virtual work, one can derive the relation between the nodal displacements and nodal forces. Since the membrane material is assumed to be volume-incompressible and initially isotropic, the strain energy function is a symmetric function of the principal stretch ratios and is only a function of in-plane stretch ratios. Therefore one can find the nodal forces in the local system as:

$$\{F_x^L\} = V_e\left(\frac{\partial W}{\partial \lambda_1}\frac{\partial \lambda_1}{\partial u^L} + \frac{\partial W}{\partial \lambda_2}\frac{\partial \lambda_2}{\partial u^L}\right), \tag{15}$$

$$\{F_y^L\} = V_e\left(\frac{\partial W}{\partial \lambda_1}\frac{\partial \lambda_1}{\partial v^L} + \frac{\partial W}{\partial \lambda_2}\frac{\partial \lambda_2}{\partial v^L}\right), \tag{16}$$

where $V_e$ is the original area of the element, $u$ and $v$ are the $x$- and $y$-component of the displacements. These nodal forces in local system are transferred back to the global system and a summation is made over all elements that meet at one node. The opposite of the resulting force is the elastic force that is implemented on fluid nodes by membrane. More details of this procedure can be found in [38,39].

## 3. Results and discussion

The present results are related to the flow geometry of deformation of an initially spherical capsule located in the middle of an unbounded shear flow (illustrated in Figure 4) with velocity $\vec{V_s} = (\dot{\gamma} y, 0, 0)$ in which $\dot{\gamma}$ is shear rate and $y$ is distance from center of the

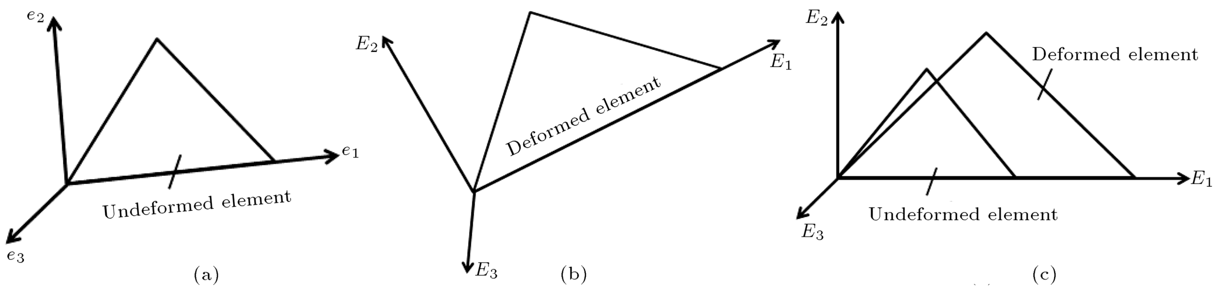


**Figure 3.** Undeformed (a) and deformed (b) triangular elements in space along with their superposition (c) shown in the deformed plane.

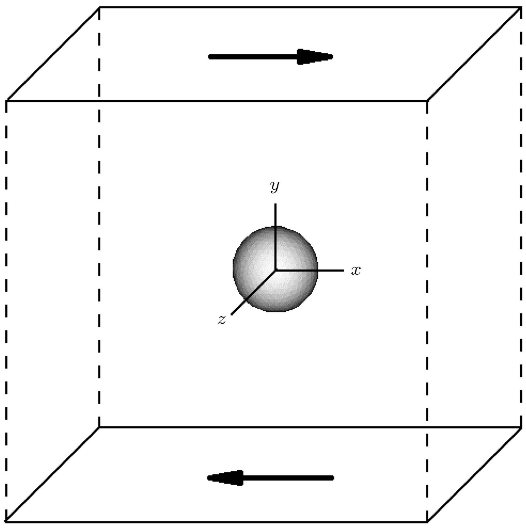


**Figure 4.** Schematic illustration of an initially spherical capsule in an unbounded shear flow.

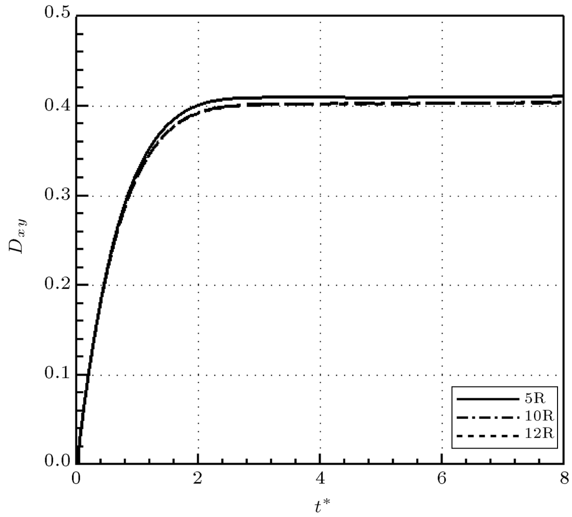


**Figure 5.** Effect of the size of computational domain on transient evolution of Taylor deformation parameter at $G = 0.1$ and $\mathrm{Re} = 0.025$ for a sphere with 1280 elements (642 nodes).

computational domain. The computational domain is a cubic box whose top and bottom walls move with the equal velocity in opposite directions to produce a simple shear flow and follow the no-slip boundary condition. In order to simulate an unbounded shear flow, the periodic boundary condition is applied at the four other boundaries of the domain to reach repeating flow conditions. Fluids inside and outside the capsule are considered as Newtonian with the same density and viscosity. No bending resistance is considered for the capsule membrane. Two dimensionless parameters affecting such flow configuration are Reynolds number, $\mathrm{Re} = \rho\dot{\gamma}R^2/\mu$, and dimensionless shear rate, $G = \mu\dot{\gamma}R/E_s$ which express the ratio of viscous force to elastic force. Here, $\rho$ and $\mu$ are the density and dynamic viscosities of surrounding fluid, respectively, $R$ is capsule radius, and $E_s$ is the membrane shear elasticity. The present study was performed at $\mathrm{Re} = 0.025$ which corresponds to Stokes flow regime. Starting from its spherical shape, membrane starts to deform gradually, changing to an ellipsoidal shape with its major axis having an angel of $\theta$ with respect to the flow direction ($x$). Capsule deformation can be represented by Taylor deformation parameter which is defined as:

$$D_{xy} = \frac{L_1 - L_2}{L_1 + L_2}. \tag{17}$$

Here, $L_1$ and $L_2$ are the largest and the smallest semi-axes of the ellipsoid with the same inertia tensor as the capsule. Using the inertia tensor in the form of [12]:

$$I^d = \int_V [r^2 I - xx] d^3 r = \frac{1}{5} \int_{\partial V} [r^2 I x - xxx].n d^2 r, \tag{18}$$

one can find the principal directions and the principal moments of the tensor ($I_i^d$) and compute the major axes of the ellipsoid ($L_i$) as:

$$I_1^d = \frac{1}{5}\rho V(L_2^2 + L_3^2), \qquad I_2^d = \frac{1}{5}\rho V(L_1^2 + L_3^2),$$

$$I_3^d = \frac{1}{5}\rho V(L_1^2 + L_2^2). \tag{19}$$

The first concern in numerical simulation of shear flow over a spherical capsule is selecting an appropriate minimum size for the computational domain. The length of the computational domain in $x$-, $y$- and $z$-directions is generally expressed based on the radius of the sphere. In order to investigate the effect of the distance between shear-producing plates, $H$, on the present computation, Taylor deformation parameter is plotted for $H$ equals to 5R, 10R and 12R in Figure 5. In this figure $t^*$ is the dimensionless time defined as $\dot{\gamma}t$. As is observed from this figure, computed values of Taylor deformation parameter for $H$ = 10R and 12R correspond to each other compared to a slightly smaller values for $H$ = 5R. Despite small difference between results obtained from $H$ = 5R and $H$ = 10R, the latter one was used in the present computations to better compare the results with previous published works with $H$ = 10R. It should be mentioned that sphere radius is selected as 6 lattice units (lu) in the present calculations which results in a computational domain of $60 \times 60 \times 60$.

The number of elements on membrane surface is another important factor which affects the accuracy of the results and computational time considerably. In creating membrane mesh, homogeneity and isotropy are two important factors which need to be considered. As implemented by many researches [16,17], a uniform and symmetric mesh can be generated starting from a

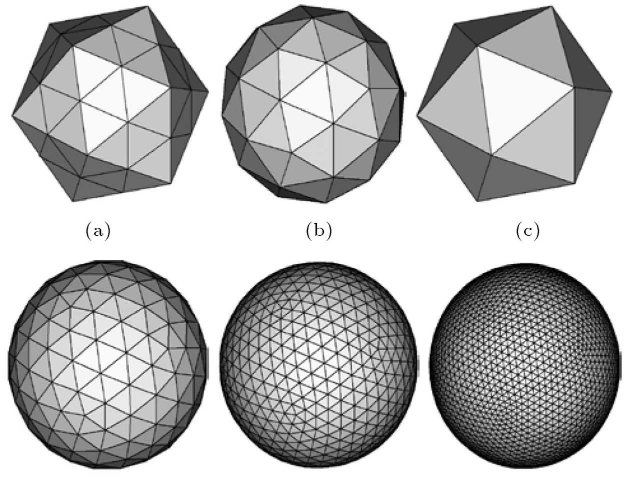


**Figure 6.** Different steps of mesh subdivision on the surface of a sphere for generating triangular elements: (a) A regular icosahedron; (b) split each face of icosahedron; (c) project each new vertex on the surface of the sphere; (d) a sphere with 162 nodes and 320 elements; (e) a sphere with 462 nodes and 1280 elements; and (f) a sphere with 2562 nodes and 5120 elements.

regular icosahedron (Figure 6(a)), which is a polyhedron with 20 identical equilateral triangular faces, 30 edges and 12 vertices. The process starts with splitting each edge of the triangular faces of the icosahedron into two equal parts (Figure 6(b)). The next step is to project the new vertices on the surface of the sphere (Figure 6(c)). This procedure is repeated until a desired resolution is obtained (Figure 6(d)-(f)).

In order to show the effects of different mesh resolutions of sphere on the accuracy of results, variation of Taylor deformation parameter is represented in Figure 7 for three sets of membrane elements. The required time for each iteration of different resolutions at $H = 10$R is also tabulated in Table 1. Based on these results, it is concluded that using a sphere with 1280 elements and 642 nodes is appropriate for obtaining accurate and efficient modeling. Moreover, Table 1 shows that increasing the number of nodes on sphere has much less effect on iteration time as compared to increasing the domain size. It should be mentioned that all of the present computations were done using a Core-i7/2.4 GHz computer.

It should be noted that the required number of membrane nodes and domain size used in the present computations are considerably smaller than those used

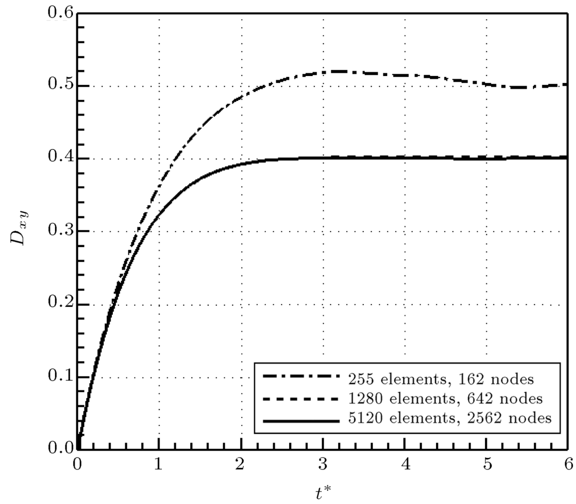


**Figure 7.** Effect of different sphere grid resolution on transient evolution of Taylor deformation parameter at $G = 0.1$ and $H = 10R$.

in previous works, such as Li and Sarkar [12], which used a computational grid of $96 \times 96 \times 48$ nodes with 5120 elements and 10242 nodes for a membrane, Doody & Boghchi [7] with a computational grid of $120 \times 120 \times 120$ nodes and 1280 elements on a membrane, and Sui et al. [13] who used multi-block technique with 8192 elements and 4098 nodes on a membrane.

As a main criterion for evaluating the results, Figure 8 shows the evolution of Taylor deformation parameter, $D_{xy}$, and inclination angle, $\theta/\pi$, with dimensionless time for a spherical capsule with membrane constitutive equation of zero-thickness shell, in shear flow at different dimensionless shear rates, $G$. The well-known behavior of initial increase followed by a steady value for Taylor deformation parameter, and initial decrease followed by a steady value of inclination angle with increasing dimensionless shear rate are clearly observed in this figure. Results of Ramanujan and Pozrikidis [4], which were obtained using boundary element method, are shown in this figure too. Close agreement between the present results and those of Ramanujan and Pozrikidis reveals the accuracy of the computational method along with its required resolution.

When a spherical capsule is exposed to the shear flow, it starts to elongate until an equilibrium state is reached. At this stage, the capsule is no longer deformed and starts to rotate around the interior fluid. The transient shapes of the deformable spherical

**Table 1.** The required time for one complete iteration in different test cases.

| Case | 255 elements, 162 nodes | 1280 elements, 642 nodes | | | 5120 elements, 2562 nodes |
|---|---|---|---|---|---|
| | $H = 10$R | $H = 5$R | $H = 10$R | $H = 12$R | $H = 10$R |
| **CPU time** | 0.63 | 0.064 | 0.67 | 1.14 | 0.76 |

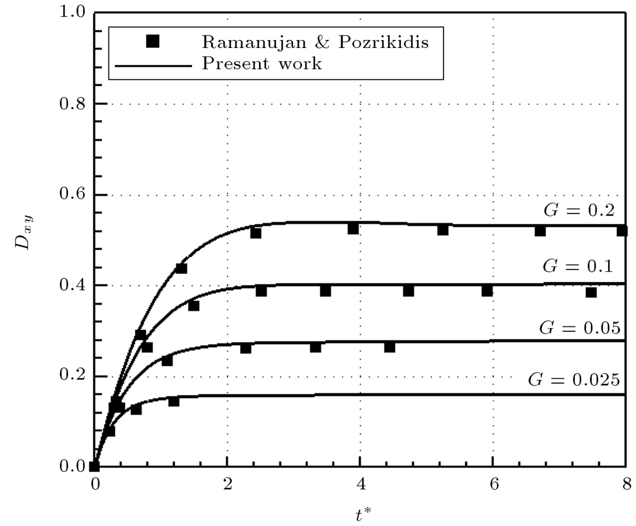


(a)

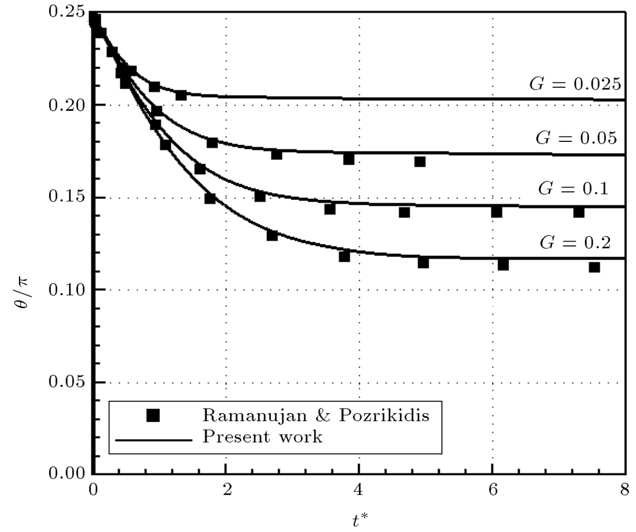


(b)

**Figure 8.** Comparison of transient evolution of (a) deformation parameter, and (b) inclination angle for a capsule with zero-thickness model in shear flow at different dimensionless shear rates at Re = 0.025.

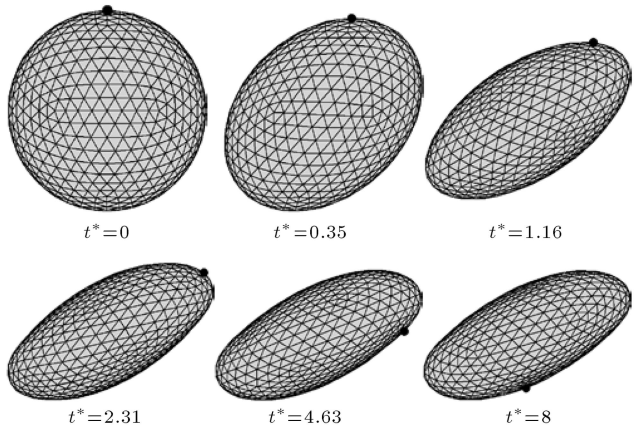


**Figure 9.** Deformation of an initially spherical capsule exposed to simple shear flow at different times; $G = 0.1$ and Re = 0.025..

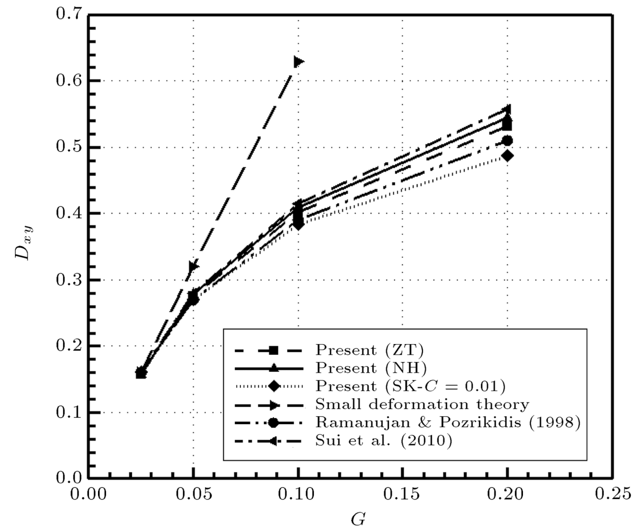


(a)

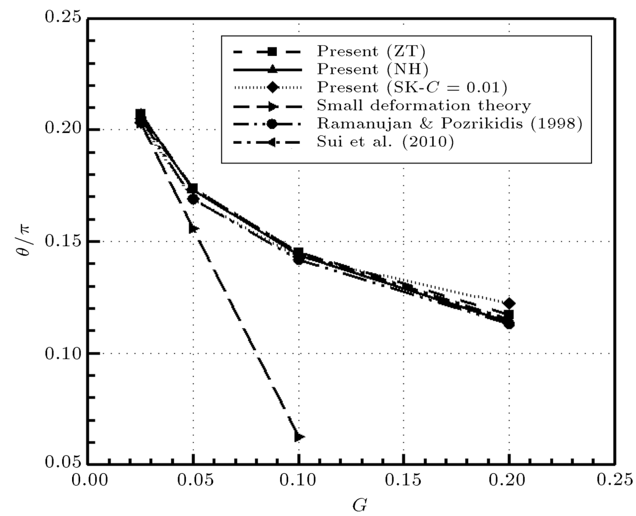


(b)

**Figure 10.** Effect of different constitutive equations on (a) a steady deformation parameter, and (b) steady inclination angle at different G.

capsule at different stages and $G = 0.1$ are shown in Figure 9. The first three figures show transient deformation and alignment of the capsule, while the last three ones represent steady deformed shapes that align with a fixed angle with respect to the $x$-axis. A material point is shown in these figures which represents tank trading motion of the membrane in the last three figures; a continuous rotation of a membrane around its steady shape.

To investigate the effect of constitutive equations on the results, three most important models, namely Zero-Thickness shell formulation (ZT), Neo-Hookean law (NH) and Skalak's law (SK) were implemented and compared in the present computations. Figure 10(a) and (b), respectively, show steady deformation parameter and steady inclination angle for different values of $G$. The results of Ramanujan and Pozrikidis [4], Sui et al. [13] and small deformation theory of Barthès-Biesel and Rallison [1] are also included in these figures for comparison. Excellent agreement is observed between present computations and those obtained from small deformation theory for $G = 0.025$. It is worth mentioning that small deformation theory is not valid at relatively large deformations, e.g. for $G \geq 0.05$. Among these three membrane laws, the ZT model predicts the closest values to those of Ramanujan and Pozrikidis [4] who used the same model. As observed from Figure 10, the aforementioned three membrane laws produce nearly equal values of $D_{xy}$ (and $\theta$) for $G \leq 0.05$ which reveals their accuracy at small deformations. This trend is not observed for relatively larger deformations. In accordance with the results of Ramanujan and Pozrikidis [4], the predicted results by ZT shell law is 1.7% and 2.4% less than those obtained by NH law for $G = 0.1$ and 0.2, respectively. It should also be noted that SK law underestimates the values of $D_{xy}$ and $\theta$, slightly, compared to the ones obtained by Ramanujan and Pozrikidis [4]. In other words, using SK membrane law results in less deformation compared to ZT or NH membrane law for the same shear rate. Such behavior for SK law is reasonable due to its strain hardening behavior. In fact, resistance to area compression in SK law prevents further deformation of the capsule which, in turn, affects the alignment of the membrane and increases the inclination angle with respect to the flow direction ($x$-axis).

One important issue in the present computations is the effect of grid uniformity on the results as compared to the published results obtained from nonuniform grid distribution. Sui et al. [13] whose computations were based on IBM/LBM/FEM, used multi-block technique for increasing concentration of grid points near the membrane. They divided the computation domain into two blocks: the interior one which is a cubic box with length of 4R around the membrane and has fine mesh with grid resolution of $\Delta x_f = \Delta y_f = \Delta z_f = R/12$, and the exterior one with the coarse mesh and grid resolution $\Delta x_c = \Delta y_c = \Delta z_c = R/6$. The present computations were done with a uniform grid with resolution $R/6$ in all directions for the whole computational domain. As observed from Figure 10(a) and (b), results of present computations are in good agreement with those of Sui et al. [13] using multi-block method. It is concluded that the condition of local grid refinement can be relaxed without losing considerable accuracy.

As mentioned before, when a capsule passes through the transient stage and reaches the steady state behavior, the material points on the membrane start to rotate along a fixed trajectory on the steady deformed shape (see Figure 9). At this level, there is no normal velocity for the membrane nodes and only tangential velocity is experienced by those nodes. This well-known periodic motion is called "tank-treading-motion". To reveal the characteristics of this motion, the position of a material point, which is initially on the top of the sphere, is plotted versus time in Figure 11 for different values of $G$ with ZT shell formulation for the membrane. The periodic motion of this material point is evident in these figures. With increasing dimensionless shear rate, $G$, the capsule elongates more which results in a larger path of rotation of the material point and its subsequent longer periodic time.

Following the position of a material point for a long time, one can find the tank-treading period $\dot{\gamma}T$ of the membrane. The tank-treading period is plotted in Figure 12 as a function of $G$ for different constitutive laws along with the results of the earlier works. In the present study, the tank-treading period is computed by following a marker point and measuring the time period for one complete cycle. Due to larger deformation and longer rotation path at higher $G$, the tank-treading period increases with increasing $G$. Results obtained from the present computations are in a reasonable agreement with those of Ramanujan and Pozrikidis [4] and Lac et al. [5] for $G < 0.1$. However, closer agreement is observed between present computations and those of Ramanujan and Pozrikidis [4] for $G = 0.2$ using ZT and NH laws. At small deformations the three constitutive equations show similar behavior and predict approximately the same value for the tank-treading period. However, at large deformation, the SK law predicts the smallest value among them. The strain hardening behavior of the SK law leads to smaller deformation and shorter rotating path, compared with other laws, which results in an underestimation. At $G = 0.2$, the predicted result by ZT law is 3% less than that obtained using NH law.

The steady shape of the deformable capsule is represented in Figure 13 for different values of $G$. Viscous forces become relatively stronger than elastic forces with increasing $G$ which results in more deformation and less inclination angle with respect to the $x$-axis.

Surface area of a deformable capsule in shear flow might not remain constant. Investigation of this effect is of prime importance in RBC deformation. To reveal the effect of shear rate on surface area and lengths of the major and minor axes of capsule, a series of computations were carried out for different dimensionless shear rates, and their results are illustrated in Figure 14(a), (b) and (c). In these figures, time variation of these parameters is expressed in nondimensional forms; lengths and area are divided by their corresponding values for the undeformed initial sphere. Figure 14(a) shows variation of major axis elongation with time. Opposite behavior is observed for the length of the minor axis of the capsule; it reduces

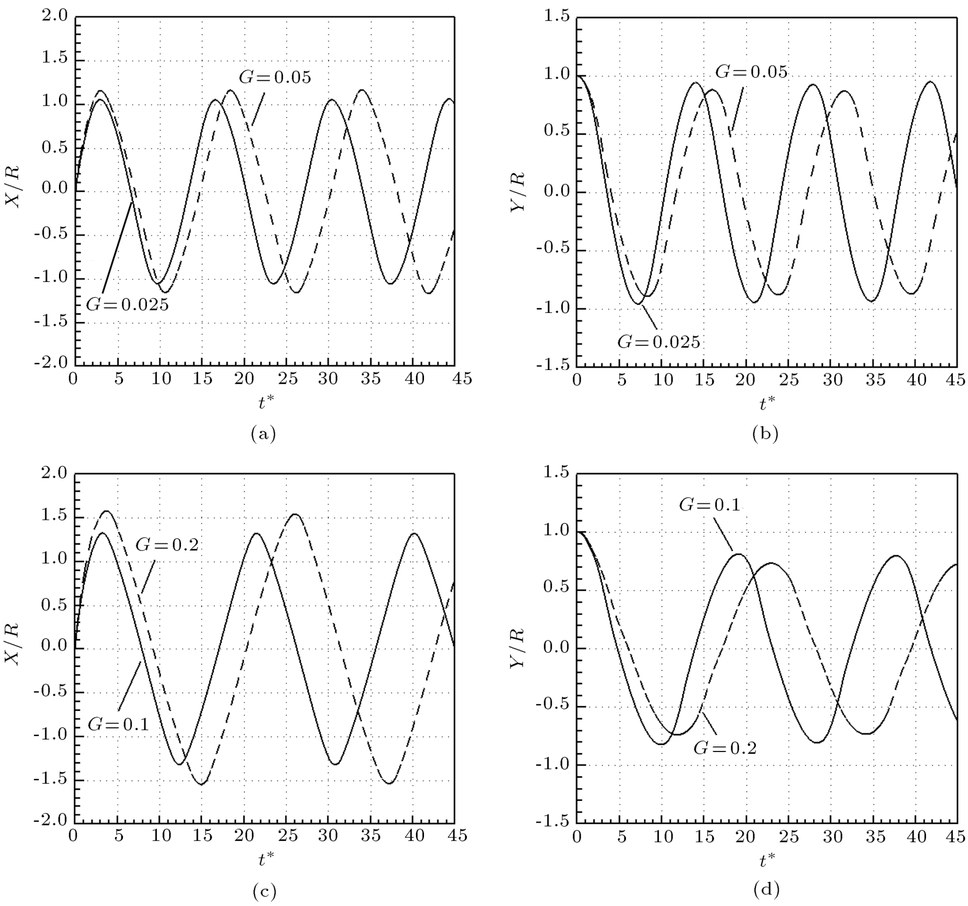


**Figure 11.** Time evolution of the position of a material point on a ZT membrane surface.

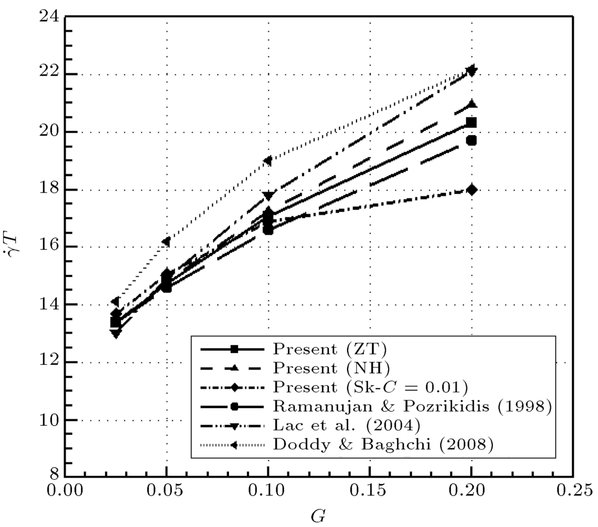


**Figure 12.** Comparison of tank-treading period for different G and different constitutive equations with earlier works.

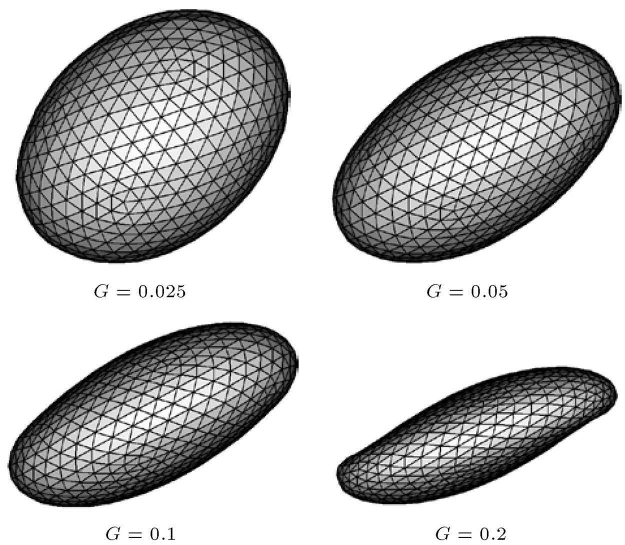


**Figure 13.** Steady deformed shape of the capsule in the plane of shear at different G and Re = 0.025.

with both increasing time and dimensionless shear rate. At equilibrium state, both lengths reach some constant values. As is observed from Figure 14(c), surface area of capsule increases with time, reaching a steady value which increases with increasing $G$. According to Figure 14(a)-(c), results obtained by ZT, NH and SK laws correspond to each other for small deformation ($G \leq 0.05$). For $G = 0.2$, the steady area of SK law is about 3.1% and 4.6% less than that for ZT and NH capsules. Unlike the SK law, at the same $G$, the NH

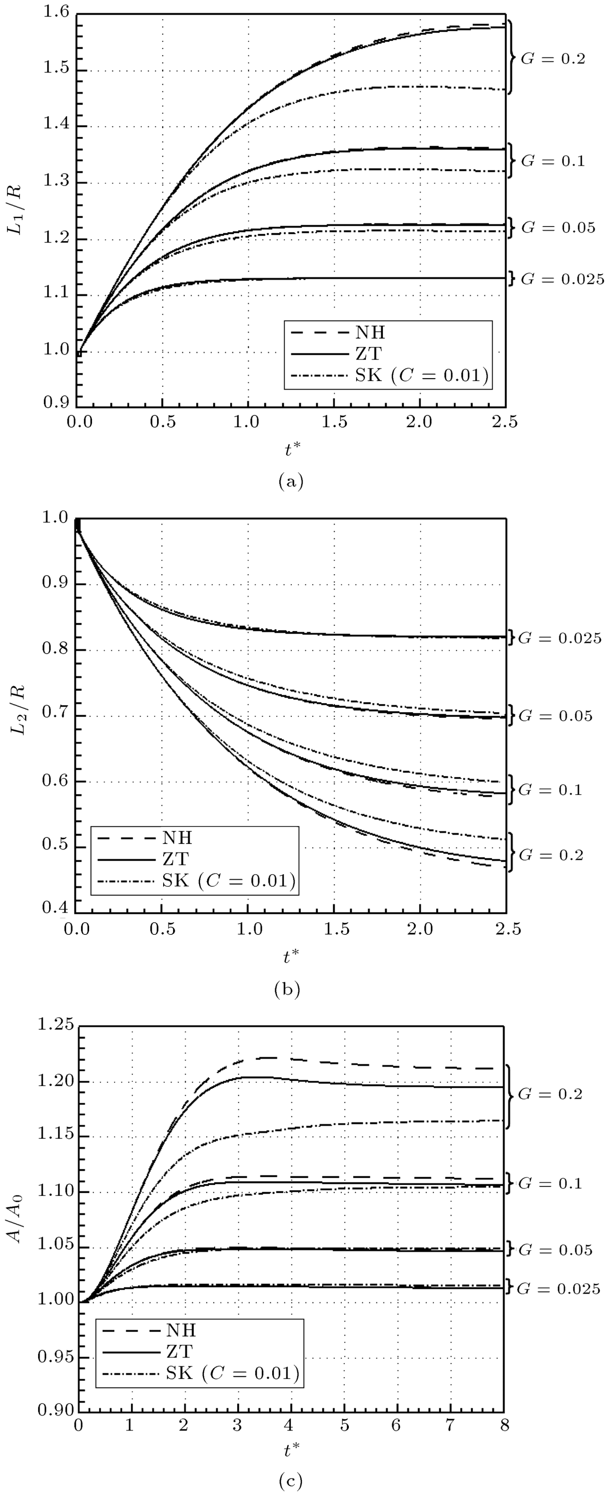


**Figure 14.** Effect of different constitutive equations on a) the lengths of major axes, b) lengths of minor axes, and c) area ratio at different G.

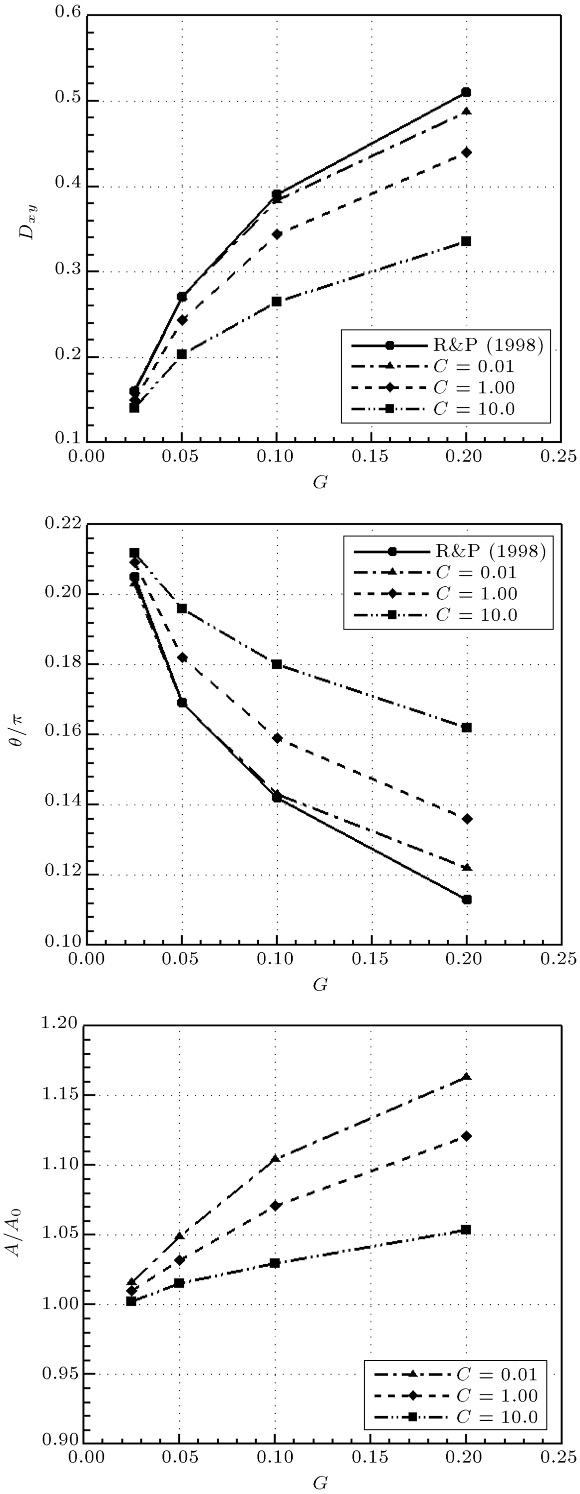


**Figure 15.** Effect of different values of coefficient $C$ on a) the Taylor deformation parameter, b) an inclination angle, and c) area ratio in SK law at different C.

law makes the biggest changes in the capsule area which shows its strain-softening behavior.

At the end of this section the effect of different values of the coefficient $C$ in SK law is investigated. The variations of deformation parameter, inclination angle and area ratio with dimensionless shear rate for different values of $C$ are plotted in Figure 15. Results of Ramanujan and Pozrikidis [4] which were obtained for a membrane with ZT shell formulation is also added to Figure 15(a) and (b). The SK constitutive equation was proposed to describe the elastic behavior of red blood cell membranes. A red blood cell tends to deform easily at a constant area. In the SK law, the resistance of the membrane to area changes is represented by coefficient $C$. If this coefficient approaches infinity, a membrane with zero change in the area is obtained. However, the behavior of SK law with small value of $C$ is close to the behavior of a ZT or NH membrane. A membrane obeying the SK law with larger values of $C$ has a larger area dilation modulus and becomes more area incompressible and less deformed at a constant shear rate. According to Figure 15(c) with $C = 10$, the final area change for $G = 0.025$, 0.05, 0.1 and 0.2 is about 0.002, 0.015, 0.03 and 0.054, respectively. With increasing the value of $C$, the inclination angle, with respect to $x$-axis, increases.

## 4. Conclusions

A three-dimensional numerical simulation is performed to study the dynamic behavior of an initially spherical capsule in simple shear flow. Fluid flow, fluid-membrane interaction and membrane analysis were studied using Lattice Boltzmann method, immersed boundary method and finite element method, respectively. Membrane analysis was done using three different constitutive equations consisting of Neo-Hookian law, zero-thickness shell approximation and Skalak's law with different area-dilation modulus. Comparison of results, in the form of Taylor deformation parameter and capsule inclination angle, showed negligible variation using different constitutive laws for $G < 0.05$ while more discrepancies were observed for $G = 0.1$ and 0.2. Results of membrane area variation during capsule deformation showed that area conservation is a good assumption for small $G$, namely $G < 0.05$, no matter which constitutive model is used for the membrane. Such behavior was not observed for $G =$ 0.1 and 0.2, and more discrepancies appeared using different constitutive laws. Using different values of the parameter, $C$, in SK model (see Eq. (14)) in computation of Taylor deformation parameter, inclination angle and area ratio showed that SK model is sensitive to such variations; good correspondence with previous published results of Ramanujan and Pozrikidis [4] could be obtained for $C = 0.01$ for small $G$ values. For $C = 10$, the maximum area change is about 5%, so since higher values of this parameter may lead to numerical instability, it seems that $C = 10$ is large enough that one can ignore the area change during the deformation. In comparison with previous techniques available in the literature the combined method can predict accurate results at low computational cost, and according to the intrinsic features of lattice Boltzmann method in parallelization processes, this method has a great capability in simulating biological problems with large number of deformable cells.

### Nomenclature

| | |
|---|---|
| $c$ | Lattice speed |
| $C$ | A coefficient in Skalak's law |
| $c_s$ | Speed of sound |
| $e_\alpha$ | Discrete velocity vector |
| $D_{xy}$ | Taylor deformation parameter |
| $E_s$ | Shear elasticity modulus |
| $f_\alpha$ | Density distribution function |
| $f_\alpha^{eq}$ | Equilibrium density distribution function |
| $F_\alpha$ | External force |
| $f$ | Eulerian external force density |
| $F$ | Lagrangian force |
| $G$ | Dimensionless shear rate |
| $H$ | Domain height |
| $I^d$ | Inertia tensor |
| $L_1, L_2$ | Semi-axes of ellipsoid |
| $N$ | Shape function |
| $R$ | Capsule radius |
| $s$ | Membrane node |
| $t$ | Time |
| $t^*$ | Dimensionless time |
| $\vec{u}$ | Fluid velocity vector |
| $U$ | Velocity of Lagrangian node |
| $u, v$ | Displacement |
| $V$ | Volume |
| $V_e$ | Original area of element |
| $W$ | Strain energy function |
| $x, y, z$ | Eulerian position coordinates |
| $X, Y, Z$ | Lagrangian position coordinates |

#### *Greek symbols*

| | |
|---|---|
| $\dot{\gamma}$ | Shear rate |
| $\delta(x)$ | Dirac delta function |
| $\theta$ | Inclination angel |
| $\lambda$ | Principal stretch ratio |
| $\mu$ | Fluid dynamic viscosity |
| $\nu$ | Fluid kinematic viscosity |
| $\rho$ | Density |
| $\tau$ | Dimensionless relaxation time |
| $\omega_\alpha$ | Weighting factor |

#### *Subscripts/superscripts*

| | |
|---|---|
| $\alpha$ | Lattice direction |

| | |
|---|---|
| *eq* | Equilibrium state |
| *L* | Local system |
| $\rightarrow$ | A vector |

## References


1. Barthès-Biesel, D. and Rallison, J.M. "The time-dependent deformation of a capsule freely suspended in a linear shear flow", *J. Fluid Mech.*, **113**(1), pp. 251-267 (1981).
2. Pozrikidis, C. "Finite deformation of liquid capsules enclosed by elastic membranes in simple shear flow", *J. Fluid Mech.*, **297**(1), pp. 123-152 (1995).
3. Zhou, H. and Pozrikidis, C. "Deformation of liquid capsules with incompressible interfaces in simple shear flow", *J. Fluid Mech.*, **283**(1), pp. 175-200 (1995).
4. Ramanujan, S. and Pozrikidis, C. "Deformation of liquid capsules enclosed by elastic membranes in simple shear flow: large deformations and the effect of fluid viscosities", *J. Fluid Mech.*, **361**, pp. 117-143 (1998).
5. Lac, E., Barthés-Biesel, D., Pelekasis, N.A. and Tsamopoulos, J. "Spherical capsules in three-dimensional unbounded Stokes flows: effect of the membrane constitutive law and onset of buckling", *J. Fluid Mech.*, **516**, pp. 303-334 (2004).
6. Barthès-Biesel, D. "Modeling the motion of capsules in flow", *Curr. Opin. Colloid Interface Sci.*, **16**(1), pp. 3-12 (2011).
7. Doddi, S.K. and Bagchi, P. "Lateral migration of a capsule in a plane Poiseuille flow in a channel", *Int. J. Multiphase Flow*, **34**(10), pp. 966-986 (2008).
8. Kwak, S. and Pozrikidis, C. "Effect of membrane bending stiffness on the axisymmetric deformation of capsules in uniaxial extensional flow", *Phys. Fluids*, **13**, pp. 1234-1242 (2001).
9. Pozrikidis, C. "Effect of membrane bending stiffness on the deformation of capsules in simple shear flow", *J. Fluid Mech.*, **440**, pp. 269-291 (2001).
10. Barthès-Biesel, D. "Motion of a spherical microcapsule freely suspended in a linear shear flow", *J. Fluid Mech.*, **100**(04), pp. 831-853 (1980).
11. Doddi, S.K. and Bagchi, P. "Effect of inertia on the hydrodynamic interaction between two liquid capsules in simple shear flow", *Int. J. Multiphase Flow*, **34**(4), pp. 375-392 (2008).
12. Li, X. and Sarkar, K. "Front tracking simulation of deformation and buckling instability of a liquid capsule enclosed by an elastic membrane", *J. Comput. Phys.*, **227**(10), pp. 4998-5018 (2008).
13. Sui, Y., Chew, Y.T., Roy, P. and Low, H.T. "A hybrid method to study flow-induced deformation of three-dimensional capsules", *J. Comput. Phys.*, **227**(12), pp. 6351-6371 (2008).
14. Sui, Y., Low, H.T., Chew, Y.T. and Roy, P. "Tank-treading, swinging, and tumbling of liquid-filled elastic capsules in shear flow", *Phys. Rev. E*, **77**(1), pp. 016310-016320 (2008).
15. Sui, Y., Chew, Y.T., Roy, P. and Low, H.T. "Inertia effect on the transient deformation of elastic capsules in simple shear flow", *Comput. Fluids*, **38**(1), pp. 49-59 (2009).
16. Sui, Y., Chen, X.B., Chew, Y.T., Roy, P. and Low, H.T. "Numerical simulation of capsule deformation in simple shear flow", *Comput. Fluids*, **39**(2), pp. 242-250 (2010).
17. Krüger, T., Varnik, F. and Raabe, D. "Efficient and accurate simulations of deformable particles immersed in a fluid using a combined immersed boundary lattice Boltzmann finite element method", *Comput. Math. Appl.*, **61**, pp. 3485-3505 (2011).
18. Pozrikidis, C. "Numerical simulation of the flow-induced deformation of red blood cells", *Ann. Biomed. Eng.*, **31**(10), pp. 1194-1205 (2003).
19. Kraus, M., Wintz, W., Seifert, U. and Lipowsky, R. "Fluid vesicles in shear flow", *Phys. Rev. Lett.*, **77**(17), pp. 3685-3688 (1996).
20. Navot, Y. and Sackler, B. "Elastic membranes in viscous shear flow", *Phys. Fluids*, **10**, pp. 1819-1833 (1998).
21. Diaz, A., Pelekasis, N. and Barthès-Biesel, D. "Transient response of a capsule subjected to varying flow conditions: Effect of internal fluid viscosity and membrane elasticity", *Phys. Fluids*, **12**, pp. 948-957 (2000).
22. Barthès-Biesel, D., Diaz, A. and Dhenin, E. "Effect of constitutive laws for two-dimensional membranes on flow-induced capsule deformation", *J. Fluid Mech.*, **460**, pp. 211-222 (2002).
23. Chang, K.S. and Olbricht, W.L. "Experimental studies of the deformation and breakup of a synthetic capsule in steady and unsteady simple shear flow", *J. Fluid Mech.*, **250**(1), pp. 609-633 (1993).
24. Walter, A., Rehage, H. and Leonhard, H. "Shear-induced deformations of polyamide microcapsules", *Colloid. Polym. Sci.*, **278**(2), pp. 169-175 (2000).
25. Walter, A., Rehage, H. and Leonhard, H. "Shear induced deformation of microcapsules: shape oscillations and membrane folding", *Colloids Surf., A*, **183**(1-2), pp. 123-132 (2001).
26. Peskin, C. "Numerical analysis of blood flow in the heart", *J. Comput. Phys.*, **25**(3), pp. 220-252 (1977).
27. Peskin, C.S. "The immersed boundary method", *Acta Numer.*, **11**, pp. 479-517 (2002).
28. Eggleton, C.D. and Popel, A.S. "Large deformation of red blood cell ghosts in a simple shear flow", *Phys. Fluids*, **10**(8), pp. 1834-1845 (1998).
29. Aidun, C.K. and Clausen, J.R. "Lattice-Boltzmann method for complex flows", *Annu. Rev. Fluid Mech.*, **42**, pp. 439-472 (2010).
30. Hashemi, Z., Abouali, O. and Kamali, R. "Lattice

Boltzmann simulation of gaseous flow in microchannel with rectangular grooves", in *ASME 2010 8th International Conference on Nanochannels, Microchannels, and Minichannels Collocated with 3rd Joint US-European Fluids Engineering Summer Meeting*, Montreal, Quebec, Canada (2010).

31. Hashemi, Z., Abouali, O. and Kamali, R. "Lattice Boltzmann simulation of suspended solid particles in microchannels", in *ASME 2011 9th International Conference on Nanochannels, Microchannels, and Minichannels*, Edmonton, Alberta, Canada (2011).

32. Hashemi, Z., Abouali, O. and Kamali, R. "Thermal three-dimensional lattice Boltzmann simulations of suspended solid particles in microchannels", *Int. J. Heat Mass Transfer*, **65**, pp. 235-243 (2013).

33. Feng, Z.-G. and Michaelides, E.E. "The immersed boundary-lattice Boltzmann method for solving fluid-particles interaction problems", *J. Comput. Phys.*, **195**(2), pp. 602-628 (2004).

34. Feng, Z.-G. and Michaelides, E.E. "Proteus: A direct forcing method in the simulations of particulate flows", *J. Comput. Phys.*, **202**(1), pp. 20-51 (2005).

35. Bhatnagar, P., Gross, E. and Krook, M. "A model for collision processes in gases. I. Small amplitude processes in charged and neutral one-component systems", *Phys. Rev.*, **94**(3), pp. 511-525 (1954).

36. Luo, L.-S. "Lattice-gas automata and lattice Boltzmann equations for two-dimensional hydrodynamics", Ph.D. Thesis, Georgia Institute of Technology (1993).

37. Skalak, R., Tozeren, A., Zarda, R. and Chien, S. "Strain energy function of red blood cell membranes", *Biophys. J.*, **13**(3), pp. 245-264 (1973).

38. Charrier, J.M., Shrivastava, S. and Wu, R. "Free and constrained inflation of elastic membranes in relation to thermoforming - non-axisymmetric problems", *J. Strain Anal. Eng. Des.*, **24**(2), pp. 55-74 (1989).

39. Shrivastava, S. and Tang, J. "Large deformation finite element analysis of non-linear viscoelastic membranes with reference to thermoforming", *J. Strain Anal. Eng. Des.*, **28**(1), pp. 31-51 (1993).

## Biographies

**Zahra Hashemi** received her MSc degree in Mechanical Engineering from Shiraz University, Iran. She is currently a PhD student at Mechanical Engineering Department of Shahid-Bahonar University of Kerman, Iran. Her main research interest includes numerical simulation of Biological systems such as deformation and motion of red blood cell in fluid flow using the lattice Boltzmann and finite element methods.

**Mohammad Rahnama** is Professor at Mechanical Engineering Department of Shahid Bahonar University of Kerman, Iran. He graduated from Shiraz University with a PhD degree in 1997. Since then he has been involved in fluid flow simulations. His interest in Lattice Boltzmann Method (LBM), as a strong simulation method in computational fluid dynamics, started a few years ago with LBM simulation of a microchannel flow. He recently focused on investigation of solid particles motion immersed in a fluid flow using LBM which was a starting point for simulation of deformable particles. Now, he is continuing his research on motion and deformation of red blood cells in blood flow using LBM, FEM and immersed boundary method.

**Saeed Jafari** received his BS degree from Shahid Bahonar University of Kerman, MS degree from Isfahan University of Technology and PhD degree from Shahid Bahonar University of Krman, Iran, in 2004, 2006 and 2010, respectively, all in Mechanical Engineering (Energy Conversion). He is currently Assistant Professor of Mechanical Engineering at Shahid Bahonar University of Kerman. His research interests include: mathematical and numerical modeling, computational fluid dynamics, particle science and technology, and simulation of multiphase flows and lattice Boltzmann method.